

Report on the mineralogical and geochemical
characterisation of Chaitén ash
for the assessment of respiratory health hazard

Claire J Horwell¹
Sabina Michnowicz¹
Jennifer Le Blond²

¹Institute for Hazard and Risk Research, Department of Earth Sciences, Durham University,
Science Labs, Durham DH1 3LE, UK.

²Department of Geography, University of Cambridge, Downing Place, Cambridge CB2 3EN,
UK.



Contents

Executive Summary	3
1. Introduction.....	4
1.1. Ash analysis protocol.....	4
1.2. Samples.....	5
1.3. Geological setting	6
1.4. 2008 eruption timeline.....	7
2. Analytical Methods	9
2.1 Sample analysis summary	9
2.1.1 Sample preparation	9
2.2 Bulk composition – X-ray fluorescence.....	10
2.2.1 Method.....	10
2.2.2 Results	10
2.3 Grain size analysis – Malvern Mastersizer	12
2.3.1 Method.....	12
2.3.2 Results	12
2.4 Particle Morphology – Scanning Electron Microscopy	14
2.4.1 Methods	14
2.4.2 Results	14
2.5 Crystalline silica quantification – X-ray diffraction.....	16
2.5.1 Method.....	16
2.5.2 Results	17
2.5.3 Discussion.....	18
2.6 Particle specific surface area – BET analysis	19
2.6.1 Method.....	19
2.6.2 Results	19
2.7 Particle surface reactivity – EPR analysis	21
2.7.1 Method.....	21
2.7.2 Results	22
3. Discussion and Conclusions.....	26
3.1 Particle size.....	26
3.2 Crystalline silica content.....	26
3.3 Surface reactivity.....	27
3.4 Differences among samples	27
3.4 Future hazard	27
3.5 Health message	28
3.6 Conclusions and suggested further work	28
4. Further Information.....	29
5. Acknowledgments	29
Appendix	30
A.1 Introduction	30
A.2 Method.....	31
A.3 Results	32
A.4. Discussion and Conclusion.....	34
References	35

Executive Summary

The mineralogical and geochemical characteristics of a suite of volcanic ash samples from Chaitén volcano were determined in order to assess the potential respiratory health hazard. Key results are as follows:

- **Bulk composition** analysis (XRF) of the samples showed that the samples are rhyolitic (72.5-74.5 wt. % SiO₂).
- **Grain size** analysis found the samples to be fine-grained, with similar grain size characteristics to the Soufrière Hills volcano (Montserrat), Mt St Helens (USA) and Merapi (Indonesia). The quantity of respirable (< 4 µm) particles ranged from 8.8-11.9 vol %.
- **Morphology** – the ash particles are angular, being composed of fragmented crystals and glass. It is not possible to distinguish mineralogical composition by observations of the morphology of the particles.
- **Crystalline silica** - The cristobalite content ranges from 2.2-7.4 wt. % with the highest quantities observed in ash deposited at Jacobaci. This compares with 15-17 wt. % cristobalite from the Soufrière Hills Volcano, Montserrat, which produces abundant cristobalite in its dome. Quartz quantities range from 0.5-1.9 wt. % and no tridymite was observed.
- **Surface area** – the surface area of the particles is low, ranging from 0.6–1.3 m²g⁻¹ which is in keeping with analyses from other volcanoes.
- **Surface reactivity** – all samples generated hydroxyl radicals (through an iron-catalysed reaction which can potentially be a carcinogenic and inflammatory factor in the lungs). The samples generated between 0.3-0.9 µmol m⁻² hydroxyl radicals after 30 mins. of reaction which is at the lower end of the range of results obtained previously for other volcanic ash samples.
- **Iron release** - the Chaitén samples released low amounts of iron (a measure of the iron available for surface reactions (11.5-30.5 µmol m⁻² after 7 days incubation). These results are in keeping with the rhyolitic (high silica, low iron) magmatic composition of the samples.

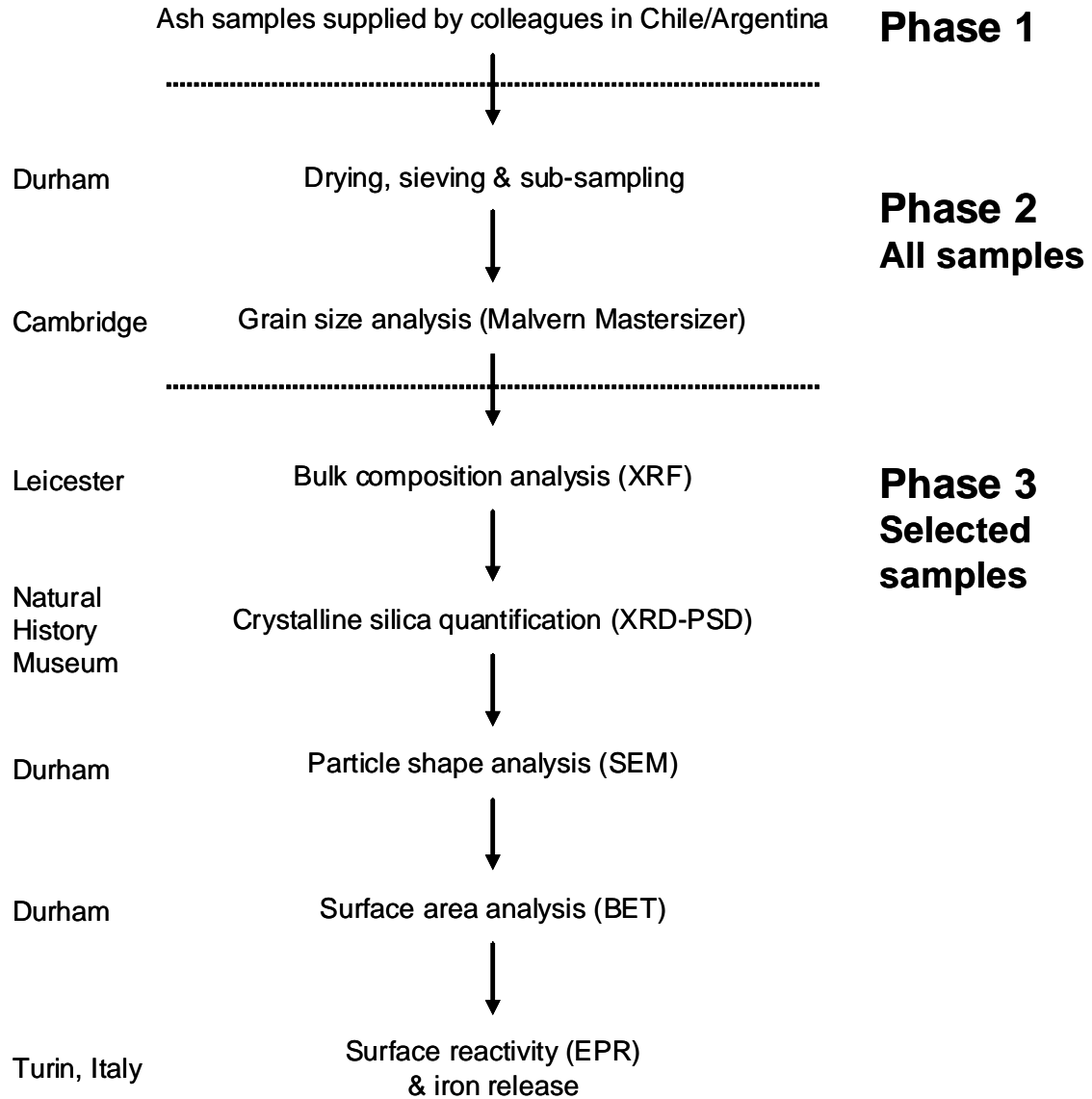
Health message

The Chaitén ash is sufficiently fine to have the potential to trigger asthma attacks in susceptible people, and aggravate respiratory symptoms in people with chronic lung problems. All people should wear masks in situations where exposure to the ash is going to be high, e.g., dry, windy days and where heavy traffic or tasks such as ash removal create dust in the air.

In public health terms, the potential for the development of long-term respiratory problems depends mainly upon the amount of crystalline silica in the ash and proportion of the ash which can be easily breathed into the deep parts of the lung. Taking these results into account and the experience acquired from other volcanoes over the last 25 years, the health hazard is low unless frequent eruptive activity commences which repeatedly exposes the population to high ash levels over long durations. In this case, careful monitoring of exposure and ash composition is required to make a full risk assessment.

1. Introduction

1.1. Ash analysis protocol



1.2. Samples

Table 1 shows the location and details of collection of the Chaitén ash samples. Figure 1 shows the location of the individual samples in relation to Chaitén volcano. Samples were sent to Durham University from SEGEMAR*, Argentina, from local government offices in Esquel[§], Argentina and from Futaleufú⁺, Chile. Information about the samples is as follows:

Table 1.2.1 Information for the samples analysed in this report

Sample No.	Eruption Date	Collection Date	Location	Grid ref.	Distance from volcano	Contamination /rain
Chai_01*	2/05/08	8/05/08	Esquel	42°54'51"S 71°19'8"W	103 km	no
Chai_02*	2/05/08	6/05/08	Jacobaci	41°33'31" S 69°52'87" W	307 km	no
Chai_03*	2/05/08	8/05/08	Trevelin	43°04'37"S 71°27'46"W	80 km	no
Chai_04*	2/05/08	8/05/08	Trevelin	43°08'21"S 71°34'03"W	80 km	no
Chai_05 [§]	2/05/08	10/05/08	Esquel	42°54'38.68"S 71°19'38.14"W	108 km	no
Chai_06 [§]	2/05/08	10/05/08	Esquel	42°54'38.68"S 71°19'38.14"W	108 km	no
Chai_07 ⁺	5/05/08	5/06/08	Futaleufú	43°10'30" S 71°45'18"W	65 km	Yes ~ 10 cm snow

[§]Chai_05 & 06 are, in fact, the same sample but were delivered in two separate bags.

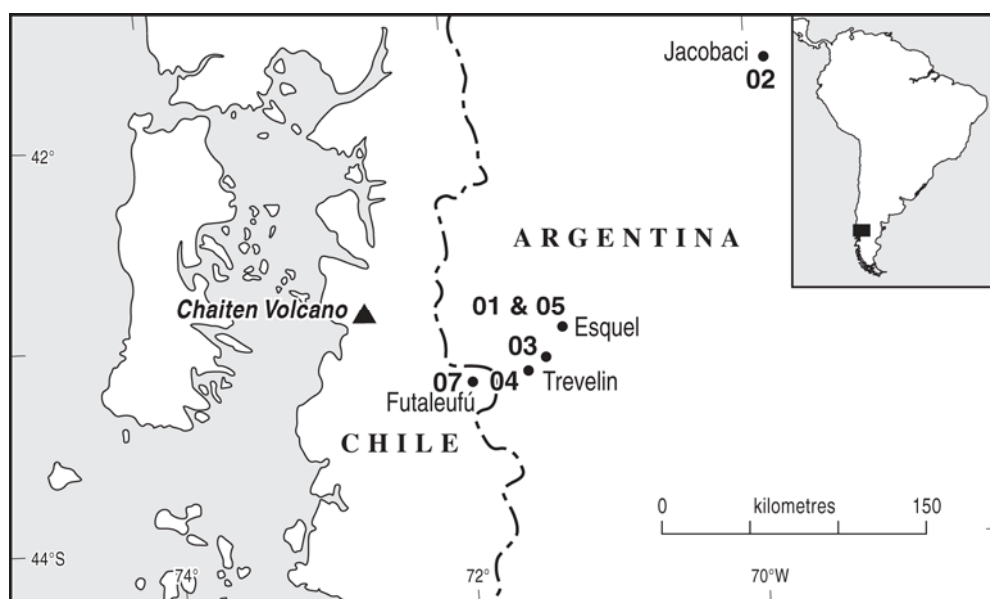


Figure 1.2.1 Location of collection of samples analysed for this report

1.3 Geological setting

Chaitén volcano, Chile, is located in the southernmost segment of the Andean Southern Volcanic Zone, which forms part of the Andean volcanic arc. The northern end of the Southern Volcanic Zone (SVZ) coincides with the locus of subduction of the Juan Fernández Ridge and the southern end with the Chile Rise. All along the SVZ, the Nazca plate is being subducted below the continent at 7-9 cm/yr. Subduction angle increases from $\sim 20^\circ$ at the northern end of the SVZ to $>25^\circ$ further to the south. As a consequence, the distance from the trench to the volcanic front decreases from >290 km in the north to <270 km in the south.

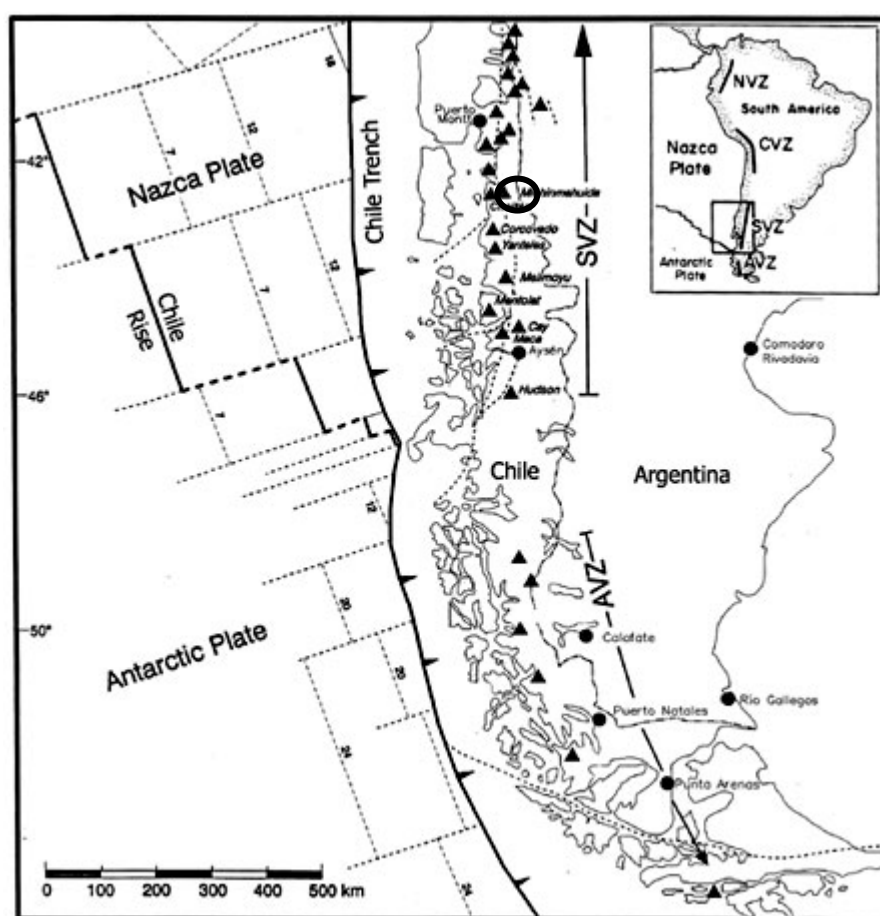


Figure 1.3.1 The Andean Southern Volcanic Zone with Chaitén volcano marked with a ring. From <http://www.scielo.cl/fbpe/img/rgch/v31n2/img03-01.jpg>

Chaitén is a small, glacier-free caldera located 10 km NE of the town of Chaitén on the Gulf of Corcovado. A pyroclastic-surge and pumice layer that is considered to originate from an eruption which formed the summit caldera has been dated to 9400 years ago. No other eruptions have been documented.

Prior to the current eruption, a rhyolitic, 962-m-high obsidian lava dome occupied much of the caldera floor. The caldera is breached on the SW side by a river that drains to the bay of Chaitén.

1.4 2008 eruption timeline

2-6 May 2008 – Plinian eruption

The first historical eruption at Chaitén began on 2 May 2008, following increased seismicity in the region on the previous day. A pulsating white-to-gray ash plume on 2 May rose to an estimated altitude of over 21 km and drifted SSE. According to news articles, Chile's government declared a state of emergency on 2 May and several hundred people were evacuated from the coastal town of Chaitén (10 km SE). Ashfall was reported during 2-6 May both locally and up to hundreds of kilometres away, affecting water supplies and roads, during 3-6 May ash plumes rose to 10.7 km altitude and drifted variably to the SE, E, W, and NE. News sources indicated that about 4,000-5,000 people were evacuated from the town of Chaitén and surrounding areas as the eruption continued. On 5 May, ONEMI (Oficina Nacional de Emergencia - Ministerio del Interior) reported that evacuations also took place in Futaleufú, about 65 km ESE of Chaitén, where ~ 30 cm of ash accumulated. One elderly person died during the evacuation efforts. On 6 May, ONEMI and SERNAGEOMIN reported that the eruption became more forceful and generated a wider and darker gray ash plume rising to an estimated altitude of 30 km (Fig. 1.4.1). All remaining people within 50 km of the volcano were ordered to evacuate.

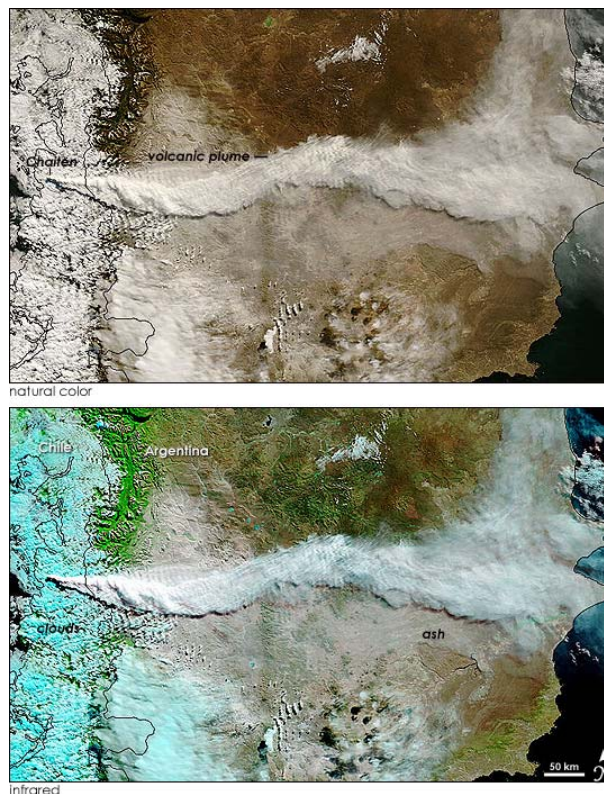


Figure 1.4.1 Satellite images on 6 May 2008 of Chaitén ash drifting and depositing over Argentina. From: http://earthobservatory.nasa.gov/NaturalHazards/natural_hazards_v2.php3?img_id=14818

6-31 May 2008 – Lava dome growth

By 21 May, aerial observations confirmed a new dome had extruded in the N-central sector of the older rhyolite dome. The new dome continued to grow through May, building on the older dome, and forming a large tephra cone. On 24 May, observers saw a vigorous eruption

venting from an explosion crater on the old dome. They also noted that the new dome had grown taller than the old one. On 26 May, reports declared that the eruption had entered a less energetic phase (subplinian) with ash plumes rising 3-5 km in altitude.

June 2008 – Ash venting and lahars

During early June ash and steam plumes rose to altitudes of up to 7 km and about 2500 hectares (6,200 acres) of forest on the N and NE flanks of the volcano were burned by pyroclastic flows or lateral explosions. The ash plumes remained at an altitude of around 3 km for the rest of June, with lahars descending multiple drainages during 27-28 June (especially notable in the Chaitén and Amarrillo rivers).

July 2008 – Dome growth and explosions

Following two weeks of inclement weather around Chaitén, visual observations on 18 July revealed mushroom-shaped ash plumes emitted from the S sector of the new lava which dome rose to an altitude of 2.5 km (8,200 ft) a.s.l. occasionally, explosions would push the plumes to altitudes of 3 km (10,000 ft) a.s.l. The plumes drifted N and NW, affecting several areas on the coast. Observations of the E-drifting eruption plume on 23 July showed it was weaker and only rose to an altitude of less than 2 km a.s.l. In contrast, during 21-23 July, earthquakes greater than M 2.6 increased in number and magnitude. On 24 July, ashfall near the city of Chaitén was about 3 cm thick and ashfall was also reported on the 27 July.

Since the initial eruption on 2 May, the volcano has emitted a near-constant plume of ash and steam.

Sources for Sections 1.3 & 1.4:

- SI/USGS Weekly Volcanic Activity Reports (sent to Volcano Listserv mailing list)
- <http://www.volcano.si.edu/world/volcano.cfm?vnum=1508-041>
- Stern, C.R., Active Andean volcanism: its geologic and tectonic setting. *Revista Geológica de Chile*, Vol. 31, No. 2, p. 161-206, 2004¹.

2. Analytical Methods

2.1 Sample analysis summary

Table 2.1.1 gives a summary of the analyses carried out on each sample. Chai_06 is identical to Chai_05 so no further analyses were carried out on Chai_06 sample.

Table 2.1.1 Analysis summary

Sample	Malvern	XRF	XRD	SEM	BET	EPR	Iron
Chai_01	√	√	√	√	√	√	√
Chai_02	√	√	√	√	√	√	√
Chai_03	√	√	√		√	√	√
Chai_04	√	√	√		√		
Chai_05	√	√	√		√		
Chai_06	√						
Chai_07	√				√	√	√

2.1.1 Sample preparation

All samples were dried in an oven set at 80°C for at least 12 hours. Samples were then sieved (Endecott stainless steel sieves) through both a 2mm and 1mm sieve in order to remove a) particles greater than 2mm diameter, which are considered larger than the volcanic ash fraction; b) particles close to 2mm which may potentially damage the Malvern Mastersizer. The samples were weighed prior to drying, following drying, and from each sieve fraction. All analyses in this report have been made on the < 1mm fraction but, as seen in Table 2.2.1, there was little sample between 1-2 mm.

Table 2.2.1 Weight (g) of ash fractions following sieving.

Sample	<1 mm	1-2 mm	> 2 mm
Chai_01	153.78	0.01	0.01
Chai_02	285.83	0.13	0.23
Chai_03	426.05	0	0
Chai_04	147.29	0.45	1.12
Chai_05	106.0	0	0
Chai_06	373.0	0	0
Chai_07	149.0	0.02	0

2.2 Bulk composition – X-ray fluorescence

When a sample is bombarded with high energy X-rays, the sample is ionised (i.e. an electron/several electrons are ejected from the atom) and becomes inherently unstable. Energy, in the form of a photon, is released as the atom strives to become stable once more. The energy released is characteristic of the atoms present. XRF is, therefore, used to determine the bulk oxide elemental composition of a sample. In turn, the bulk compositions are used to classify the type of magma erupted.

2.2.1 Method

Samples were analysed on the PANalytical Axios Advanced XRF spectrometer at the Department of Geology, University of Leicester. Major elements were determined on fused glass beads prepared from ignited powders, with a sample to flux ratio 1:10, 100% Li tetraborate flux.

2.2.2 Results

The results are quoted as a component oxide weight percent, re-calculated to include loss on ignition (LOI)(Table 2.2.1, below). Figure 2.2.1 plots the results on a total alkali-silica plot (TAS plot) in order to define the magmatic composition of the samples.

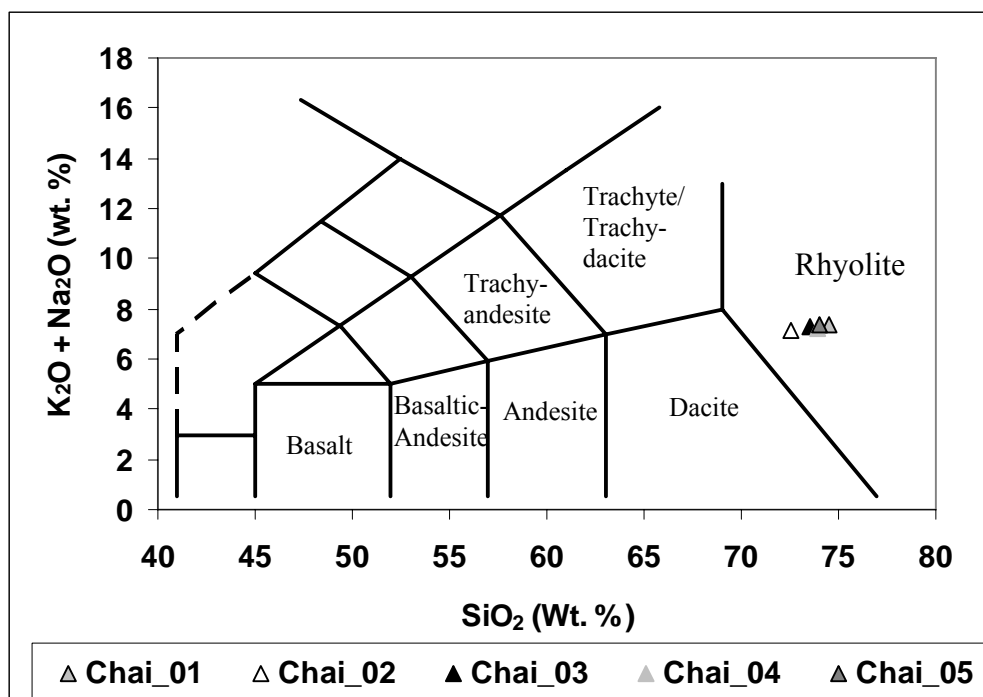


Figure 2.2.1. Results from the XRF analysis of the volcanic ash samples, plotted on a TAS (total alkali versus silica content²) plot.

Using the IUGS (International Union of Geological Sciences) classification of igneous rocks based on the alkaline content (see Fig. 2.2.1), the samples are rhyolitic.

Table 2.2.1. Results of the XRF analysis for the volcanic ash samples (wt. %)

Sample	SiO ₂	TiO ₂	Al ₂ O ₃	Fe ₂ O ₃	MnO	MgO	CaO	Na ₂ O	K ₂ O	P ₂ O ₅	SO ₃	LOI	SiO ₂	Total
Chai_01	74.49	0.16	13.97	1.54	0.055	0.27	1.53	4.33	3.028	0.063	0.01	0.74	74.49	100.18
Chai_02	72.55	0.18	13.79	1.88	0.066	0.45	1.76	4.19	2.958	0.068	0.12	1.07	72.55	99.08
Chai_03	73.54	0.16	13.92	1.62	0.057	0.33	1.59	4.29	2.989	0.064	0.02	0.86	73.54	99.43
Chai_04	73.96	0.17	13.99	1.67	0.058	0.33	1.63	4.27	2.956	0.066	0.02	0.97	73.96	100.09
Chai_05	73.98	0.15	13.79	1.53	0.055	0.22	1.50	4.31	3.048	0.060	0.00	0.67	73.98	99.31

2.3 Grain size analysis – Malvern Mastersizer

The Malvern Mastersizer 2000 is a laser diffraction particle size analyser, which measures the total number of particles within the 0.2-2000 μm range. The results are from the Malvern Mastersizer 2000 with Hydro MU attachment at the Department of Geography at the University of Cambridge.

2.3.1 Method

The < 1mm fraction was analysed on a Malvern Mastersizer 2000 with Hydro MU attachment at the Department of Geography, Cambridge University, UK. Ultrasonics were used to disaggregate samples and the results below are from an average of three runs. Samples were measured with a refractive index of 1.63 and an absorption coefficient of 0.1 (after Horwell, 2007³).

2.3.2 Results

Table 2.3.1 gives information on the potential effects of each grain size fraction. Results in Table 2.3.2 are the cumulative volume % of grain size within the health-pertinent fractions.

Table 2.3.1. Potential health effects of ash fractions.

Size	Potential Health Effect
< 4 μm	‘Respirable’ fraction – can enter the alveoli where chronic disease could occur with long-term exposure
< 10 μm	‘Thoracic’ fraction – can enter past the bronchus, where bronchitis, asthma and other acute diseases may be triggered in susceptible people.
< 15 μm	Can enter the throat, causing rhinitis, laryngitis and irritation

Table 2.3.2 Grain-size results in cumulative volume %

Size	Chai_01	Chai_02	Chai_03	Chai_04	Chai_05	Chai_06	Chai_07
< 4 μm	9.71	10.73	11.93	8.73	10.32	10.72	9.65
< 10 μm	20.23	21.60	24.35	18.13	21.39	22.47	20.76
< 15 μm	27.33	28.91	32.57	24.37	28.87	30.62	28.19

Table 2.3.3 shows results published from other volcanoes³. It can be seen that the Chaitén volcanic ash is fine-grained, with similar grain size characteristics to the Soufrière Hills volcano (Montserrat), Mt St Helens (USA) and Merapi (Indonesia). Please refer to Horwell 2007³ for further information on those eruptions. There does not appear to be a correlation in grain size with distance from the volcano.

Table 2.3.3 Grain size analyses from other volcanoes (from Horwell, 2007³)

Volcano	Magma type/ Eruption style	VEI*	Grain- size distribution, Cumulative volume %					
			< 1 µm	< 2.5 µm	< 4 µm	< 10 µm	< 15 µm	< 63 µm
Pacaya, Guatemala 1994	Basaltic Stromb.-Vulc.	1	0.00	0.00	0.04	0.41	0.70	2.23
Pacaya, Guatemala 1992	Basaltic Stromb.,-Vulc.	1	0.00	0.26	0.76	2.43	3.76	16.60
Fuego, Guatemala 1999	Basaltic Vulcanian	2	0.00	0.00	0.00	0.00	0.00	1.56
Ulawun, Papua New Guinea	Basaltic Strombolian	2	0.00	0.02	0.27	0.88	1.63	4.14
Cerro Negro, Nicaragua	Basaltic Stromb.-Vulc.	2	0.00	0.22	0.64	2.55	4.17	14.64
Tungurahua, Ecuador	Andesitic Stromb.-Vulc.	2	0.65	2.49	4.11	10.49	15.46	41.80
Langila, Papua New Guinea	Bas.-And. Vulcanian	2	0.87	3.29	5.63	13.95	19.83	52.71
Merapi, Indonesia	Bas.-And. Dome collapse	2	1.95	8.02	12.66	27.24	38.11	83.06
Vesuvius, Italy AD79-472	Teph. -Phon. Stromb.-Vulc.	2-3	0.72	2.09	3.24	7.13	10.14	33.99
Sakurajima, Japan	Andesitic Vulcanian	3	0.00	0.50	0.86	1.95	2.87	14.74
Etna, Italy	Basaltic Strombolian	3	0.27	1.09	1.83	4.59	6.75	22.17
Ruapehu, New Zealand	Andesitic Sub-plinian	3	0.51	2.44	4.14	9.43	13.37	32.19
Soufrière Hills, Montserrat 1997	Andesitic Vulc. explosion	3	1.00	3.60	5.90	13.40	18.50	44.08
Soufrière Hills, Montserrat 1999	Andesitic Dome collapse	3	1.94	6.74	10.70	23.10	31.90	76.88
Soufrière Hills, Montserrat 2003	Andesitic Dome collapse	3	2.70	7.87	11.47	22.49	30.75	74.63
Fuego, Guatemala 1974	Basaltic Subplinian	4	0.88	2.43	3.66	7.99	12.04	46.64
El Reventador, Ecuador	Andesitic Vulcanian	4	0.90	3.21	4.88	10.16	15.12	72.93
Mt St Helens, USA	Dacitic Plinian	5	1.69	7.39	11.74	24.50	33.15	78.76
Vesuvius, Italy AD79	Teph. -Phon. Plinian	5	4.81	11.62	16.93	32.83	43.39	83.70
Pinatubo, Philippines 3/6/91	Dacitic Plinian	6	1.07	5.49	8.97	17.88	23.12	54.05
Pinatubo, Philippines 4/7/91	Dacitic Sub-plinian	6	1.33	6.18	9.82	18.93	24.34	60.69

Amount of material for health-pertinent fractions found in selected samples of volcanic ash. The table is ordered by increasing VEI (volcanic explosivity index). Grain-size distributions measured on Malvern Mastersizer 2000 with Hydro MU.

2.4 Particle Morphology – Scanning Electron Microscopy

Scanning electron microscopy allows the user to observe the morphology of volcanic ash. Analysis was carried out on uncoated samples in a Hitachi TM-1000 Tabletop SEM Microscope in the Department of Earth Sciences, Durham University.

2.4.1 Methods

Stubs were assembled by sticking a carbon sticky pad on to an aluminium SEM stub. A small (0.5 mm diameter) polycarbonate disc was then stuck to the sticky pad and ash was either sprinkled or smeared (with ethanol) onto the disc. Samples were left un-coated due to instrumental problems.

2.4.2 Results

The general morphology of the ash was similar to previously-observed volcanic ash samples (see Figs. 2.4.1 and 2.4.2). The ash particles are angular, with fractured surfaces, being composed of fragmented crystals and glass. It is not possible to distinguish mineralogical composition by observations of the morphology of the particles.

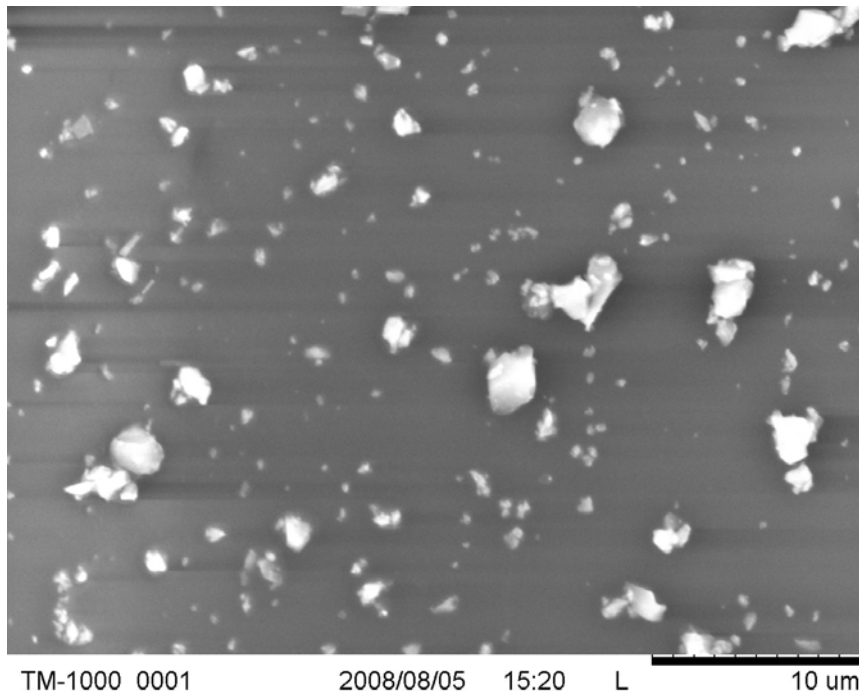
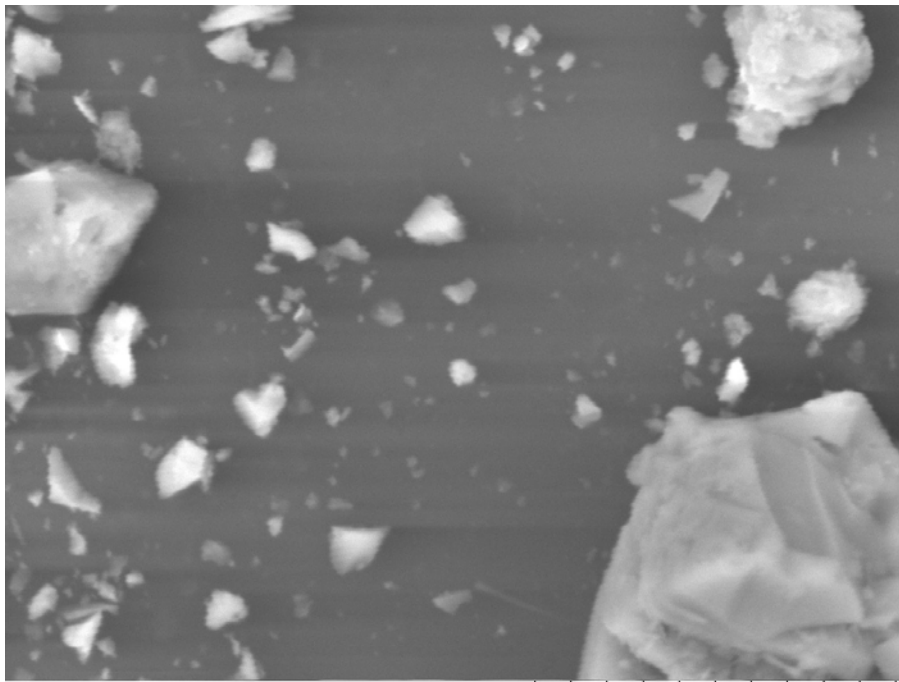


Figure 2.4.1 Scanning Electron Microscope image of Chai_01 showing a typical view of very fine-grained particles. Many of the particles are $< 1 \mu\text{m}$ diameter. Horizontal dark ‘smears’ are artefacts of charging because the sample was un-coated.



TM-1000_0006 2008/08/05 16:01 L 10 um

Fig. 2.4.2 SEM image of Chai_01 showing a typical view of fine-grained and larger particles. Horizontal dark 'smears' are artefacts of charging because the sample was un-coated.

2.5 Crystalline silica quantification – X-ray diffraction

X-ray diffraction allows the user to identify the crystalline components in a bulk powdered sample. Quantification of phases is difficult in powders of multi-mineral compositions, particularly if the mineral assemblage is not known in advance. A whole-pattern peak-fitting method has been used for volcanic ash samples previously, where the mineral assemblage was known. For lesser studies samples, it is extremely difficult to perform due to the lack of knowledge of which standard materials should be used to replicate the assemblages in the samples.

Here rapid quantification of certain phases of interest was carried out using an internal standard, following a previously-tested method (see Appendix). This IAS (Internal Attenuation Standard) method allows us to attain the wt. % of any phase within the sample without needing to know the mineralogical composition of the bulk sample.

Crystalline silica polymorphs have been singled out for quantification because they are classed as human carcinogens⁴ and may cause the fibrotic lung disease silicosis. It is still unclear whether volcanic crystalline silica can cause these diseases but until this is clarified, all health assessment studies must consider the amount of crystalline silica present. See Horwell & Baxter (2006⁵) for a full review.

It should be noted that results presented here are for the weight percent of crystalline silica polymorphs in the bulk ash sample rather than in the sub- 4 or sub-10 μm fractions. However, Horwell et al. (2001⁶) showed that crystalline silica is usually more abundant in the fine ash fractions due to fragmentation processes so we may expect the percentage of silica in the fine fractions of the Chaitén ash to be elevated relative to the results presented here.

2.5.1 Method

The samples were ground with an agate pestle and mortar, to reduce the grain size to between $\sim 5\text{-}20$ μm diameter. A small sub-sample was smeared onto a quartz substrate and analysed for the identification of the crystalline phases. An Al deep well mount was created for the quantitative experiments. XRD data were collected using an Enraf-Nonius X-ray diffractometer with an INEL curved position sensitive detector (PSD) at the Natural History Museum, London.

Radiation - Cu $K\alpha_1$
Slit size – 0.24 by 5.0 mm
 μ - 5.0
EHT – 20 kV

2.5.2 Results

i. Peak identification

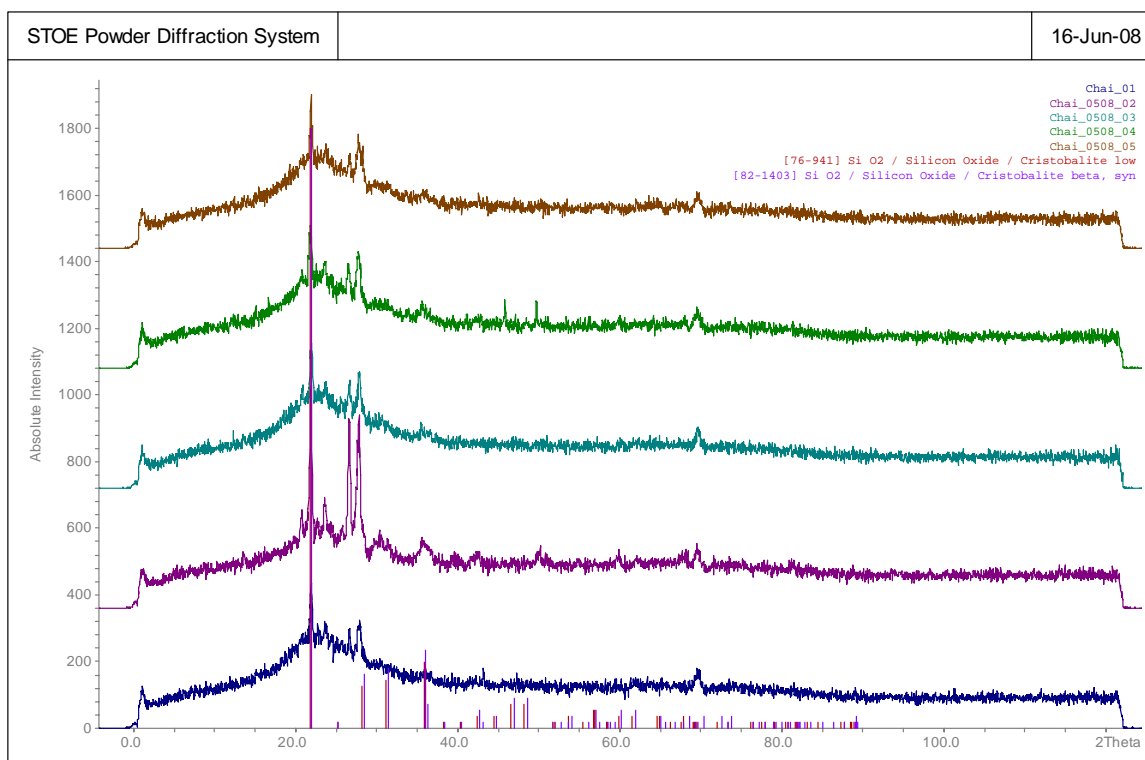


Fig. 2 XRD patterns for the five Chaiten ash samples, run for 10mins each (deep well).

ii. Quantitative data

Table 2.5.1, below, gives the quantification results for the crystalline silica polymorphs cristobalite and quartz. Tridymite was not identifiable.

Sample	Cristobalite wt. %	Quartz wt. %
Chai_01	2.21	0.67
Chai_02	7.42	1.91
Chai_03	2.77	0.58
Chai_04	2.39	0.80
Chai_05	2.80	0.58

Table 2.5.1 Results from the IAS method for quantifying phases within a sample. Results are an average of three separate 'by eye' readings. Errors are +/- 3wt. %.

Results show that the Chaitén samples all have around 2.5 wt. % cristobalite and 0.6 wt. % quartz with the clear exception of sample Chai_02 which has substantially more cristobalite and quartz than the other samples.

2.5.3 Discussion

The new IAS method has, to date, only been tested on a few volcanic samples but has been fully verified, giving accurate results during testing on synthetic mixtures of known quantities of minerals (see Appendix). To compare the results of the current samples with other volcanic samples, we also have tested ash from the Soufrière Hills Volcano, Montserrat which produces abundant cristobalite within its lava dome. The Soufrière Hills bulk dome-collapse ash contains 15-17 wt. % cristobalite both by the IAS method and by a 'peak-stripping' method which is more time-consuming and requires standards for all minerals present (see Appendix). We have also recently studied ash from Rabaul volcano in Papua New Guinea. These samples contained 2-5 wt. % cristobalite. These data are similar to the Chaitén results. The Rabaul samples are mainly andesitic but, as with Chaitén, the ash was not formed from collapse of a cristobalite-rich lava dome. In both cases, the presence of cristobalite may be related to crystallisation from hydrothermal fluids and incorporation of hydrothermally-altered rock, rather than primary magmatic effects.

2.6 Particle specific surface area – BET analysis

The specific surface area, combined with the surface reactivity, of a sample needs to be measured in order to determine the likelihood of particle toxicity within the lung. The calculation of ‘surface area x surface reactivity’ for any given sample, forms the basic model for cellular toxicity of insoluble compact particles (Prof. Ken Donaldson, pers. comm.) (see section 2.7 Particle Surface Reactivity). Particle surface area is also used for expressing dose in toxicological experiments, so knowledge of the surface area of the samples is useful if it is decided that toxicological tests are warranted at a later date.

Here we used the BET (Brunauer Emmet Teller) method of specific surface area analysis using nitrogen absorption with a Micromeritics TriStar 3000 Surface Area and Porosimetry Analyser in the Dept. of Chemistry, Durham University.

2.6.1 Method

Prior to analysis, samples were degassed at 150 °C for two hours.

2.6.2 Results

The specific surface area measured ranges from 0.6-1.3 m² g⁻¹. Chai_02 has marginally greater surface area than the other samples analysed.

Table 2.6.1. Results of the BET analysis to determine the surface area.

Sample	Specific surface area (m ² g ⁻¹)	Error (+/- m ² g ⁻¹)
Chai_01*	0.7020	0.0014
Chai_02*	1.2809	0.0027
Chai_03 [§]	0.6956	0.0013
Chai_04 [§]	0.6780	0.0013
Chai_05 [§]	0.6427	0.0014
Chai_07 [§]	0.8113	0.0016

*Result is average of three runs. [§]Result is average of two runs.

Table 2.6.2 (below) allows comparison between the Chaitén samples and published data on specific surface area from volcanoes around the world. It can be seen that the Chaitén samples have specific surface areas in keeping with other ash samples.

Table 2.6.2. Surface area of various samples of volcanic ash (from Horwell et al., 2007⁷). Surface areas were measured by the BET (Brunauer Emmet Teller) method of nitrogen adsorption (Micromeritics Gemini Analyser with Flow Prep 060).

Volcano	Surface area (m²g⁻¹)
Cerro Negro, Nicaragua	0.47
El Reventador, Ecuador	1.53
Etna, Italy	0.19
Fuego, Guatemala	0.54
Langila, Papua New Guinea	0.9
Merapi, Indonesia	1.83
Mt St Helens, USA	1.62
Pacaya, Guatemala	0.21
Pintatubo, Philipines	0.89
Sakurajima, Japan	0.97
Soufrière Hills, Montserrat 1	1.28
Soufrière Hills, Montserrat 2	1.34
Tungurahua, Ecuador	0.72

2.7 Particle surface reactivity – EPR analysis

The surface reactivity of particles is often assessed by their ability to generate free or surface radicals. Recent work on volcanic ash has focussed on iron-catalysed free radical generation which is known to be potentially both a lung inflammation factor and a carcinogenic factor^{8,9}. Radical generation can become prolonged where the iron is present in a specific oxidative and coordinative state on the surface of the particulate matter⁸⁻¹³. Although iron is usually present in the Fe³⁺ oxidative state in crustal dusts, Horwell et al. (2003¹⁴) found that volcanic ash contains abundant Fe²⁺. In the presence of hydrogen peroxide (produced naturally in the lungs), Fe²⁺ can catalyze the generation of hydroxyl radicals, through the Fenton reaction. Horwell et al. (2003¹⁴) found that andesitic volcanic ash generated abundant hydroxyl radicals (the Soufriere Hills, Montserrat ash) and Horwell et al. (2007⁷) showed that all ash types seem capable of generating hydroxyl radicals, but particularly basaltic ash (which is iron rich) which had previously been disregarded as a respiratory health hazard due to the lack of crystalline silica in these magma compositions.

Electron Paramagnetic Resonance (EPR) spectroscopy is employed for the identification of radicals on the surface of the volcanic ash. The amount of free radicals generated and released into solution can be quantified by using the spin-trapping technique^{7, 14-17}. Since samples exhibit differences in surface area, results are expressed on a per unit surface area basis (see Section 2.6) to measure the real reactivity of the surface. A Miniscope 100 ESR spectrometer, Mag-nettech at the Università degli Studi di Torino, Italy was used in these experiments.

2.7.1 Method

EPR Spin-trap

The method replicates the Fenton reaction which may occur in the lung. 150 mg of the ash sample is suspended in 500 μ L 0.5 M phosphate buffered solution at pH 7.4 (the pH of lung fluids), then 250 μ L of 0.15 DMPO (the spin trap; 5,5'-dimethyl-1-pyrroline-*N*-oxide) and 500 μ L H₂O₂ (0.2 mL 30 wt. % H₂O₂ in 10 mL H₂O) are added and the suspension stirred for 1 hour. During the 1 hour experiments aliquots of the suspension are withdrawn from a darkened vial after 10, 30 and 60 mins. and filtered through 0.25 μ m filters. The liquid is introduced into a 50 μ L capillary tube and placed in the EPR spectrometer. Each sample was tested at least twice and an average taken.

Receiver gain 9×10^2

Microwave power 10 mW

Modulation amplitude 1 G

Scan time 80 sec

Scans 2

The integrated amplitude of the peaks generated is proportional to the amount of radicals generated. The number of radicals is calculated by including a solid solution of Mn²⁺ in CaCO₃ as a calibration standard.

Iron release

Experiments were also carried out to characterise the amount of removable Fe^{2+} and Fe^{3+} from the surface of the ash as this represents the iron available for participation in the Fenton reaction (Fe^{3+} can be reduced to Fe^{2+} in the lung via the Haber Weiss cycle). Removable Fe^{2+} was measured through the use of ferrozine, a bidentate N donor chelator (pH 4) specific for Fe^{2+} , in the presence or in the absence of ascorbic acid, following a method previously described^{7, 8, 14}. Since ascorbic acid reduces Fe^{3+} to Fe^{2+} the amount of iron measured in the presence of ascorbic acid corresponds to the total iron mobilised.

Samples (each of 20 mg) were placed in tubes with 20 mL of 1 mM solutions of ferrozine or ferrozine and ascorbic acid (1 mM). The suspensions were stirred at 37 °C. After 1 d the samples were removed and centrifuged for 15 min and an aliquot of the supernatant was analysed in a Uvikon spectrophotometer (at 562 nm) as ferrozine forms a coloured complex with Fe^{2+} . The samples were then returned to the incubator and measured in this way every 24 h for 9 days. A control solution of ferrozine with water showed no colour change over the experiment. As with the EPR data, the results are expressed per unit surface area.

2.7.2 Results

Figure 2.7.1 shows the hydroxyl radical generation results over the 60 minutes of each experiment. All samples generated the hydroxyl radical over the duration of the experiment. There is no consistent relationship in the kinetics of the experiment over time among the samples, however.

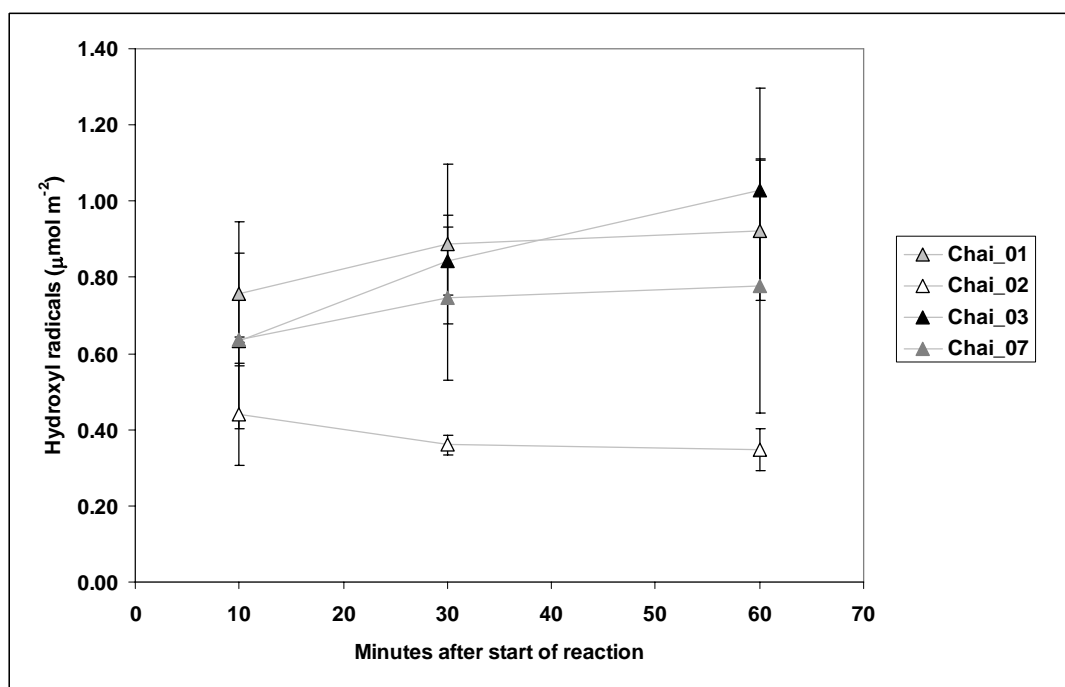


Figure 2.7.1 Production of hydroxyl radicals (per unit surface area) for the samples over the 60-minute experiments. Each value is the average of two experiments with error bars representing the standard error.

Figure 2.7.2 shows the results of the iron release experiments. As expected from the magmatic composition of the samples (Fig. 2.2.1), all of the samples displayed relatively low iron

release in comparison to basaltic samples from previously published work⁷. Chai_02 contained marginally more available iron than the other samples, however.

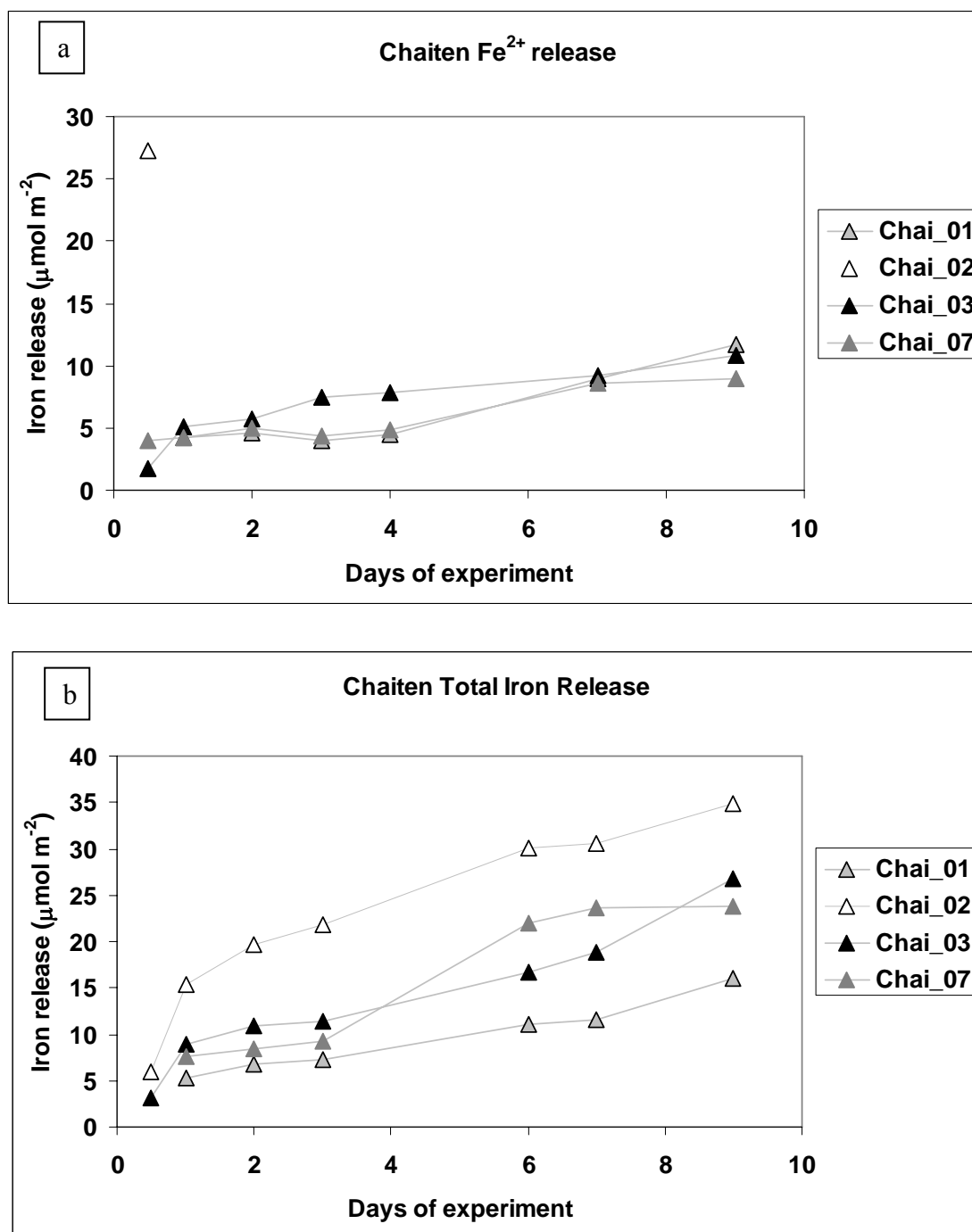


Figure 2.7.2. Amount of iron removed as a) Fe²⁺ and b) total iron during 9 days of incubation with chelators. The iron removed is expressed as amount per unit surface area. The Fe²⁺ result for Chai_02 is given for day 0 only because the experiment was aborted on day 1 due to spillage.

The correlation between the amount of hydroxyl radicals generated after 30 min of incubation and the amount of iron released (in both oxidative states) after 7 d of incubation is reported in Figure 2.7.3.

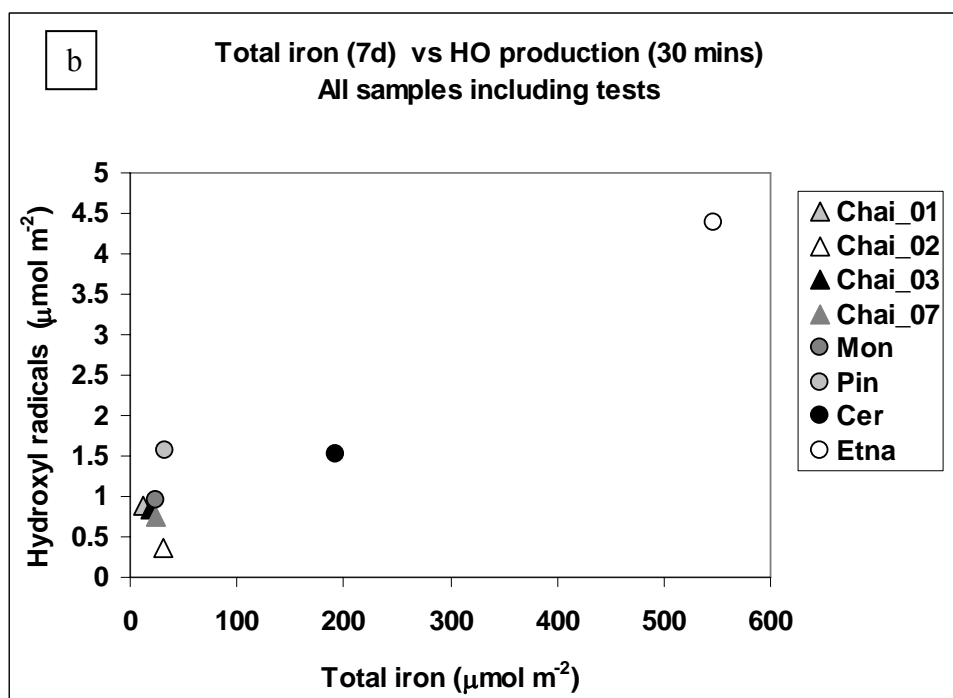
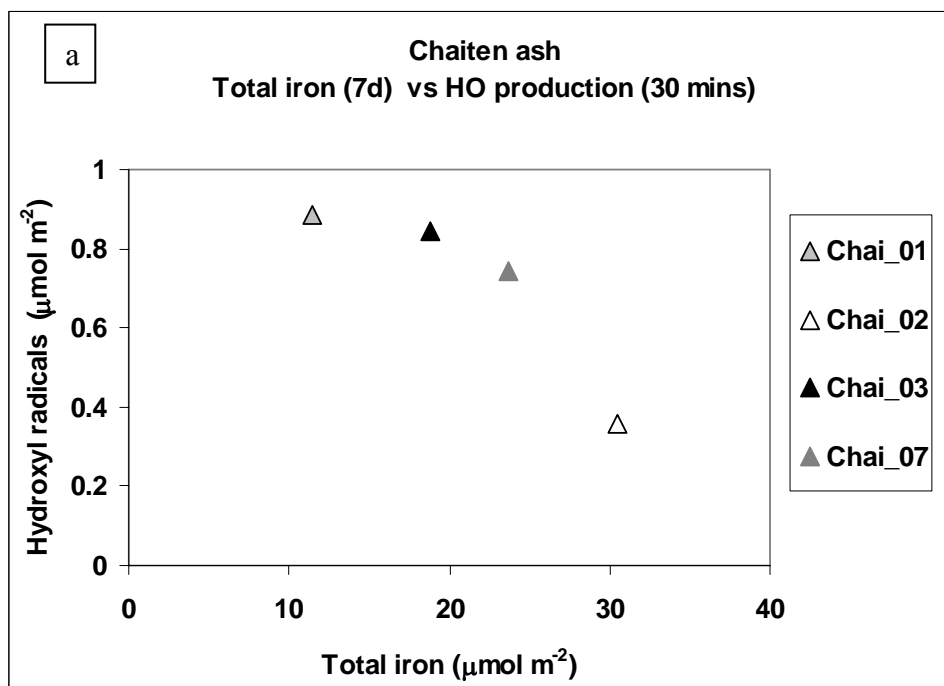


Figure 2.7.3 Amount of hydroxyl radicals generated after 30 min from the start of incubation versus total amount of iron extracted by chelators after 7 d. a) Chaitén samples; b) Chaitén samples and four samples previously used by Horwell et al. (2007). Mon = Soufrière Hills, Montserrat (5/6/99); Pin = Pinatubo (1991); Cer = Cerro Negro (1995); Etna = Mt. Etna, Sicily (2002).

Figure 2.7.3 a) shows that, for the Chaitén samples, there is no positive correlation between the amount of available iron for reaction and the number of radicals generated. To compare with previously published results, Figure 2.7.3 b) compares the Chaitén samples with four samples of ash which were previously analysed by Horwell et al. (2007⁷). Here, these samples were re-analysed to check that the current results were comparable with previously published results. The new and old data compared well. Figure 2.7.3 b) shows that the Etna and Cerro

Negro ash samples (both basaltic) were capable of generating more radicals, and have more available iron, than any of the Chaitén samples. The Chaitén samples all compare well with the andesitic Soufrière Hills, Montserrat sample. Amongst the Chaitén samples, again Chai_02 is slightly unusual, showing reduced radical generation despite increased iron availability. We also note that data for Chai_07 (although not appearing to be unusual) may be affected by the fact that this sample was collected one month after eruption and was contaminated by at least 10 cm of snowfall. Previously published results (Horwell et al. 2003¹⁴) have shown that weathered samples are less reactive and more oxidised than freshly collected samples.

3. Discussion and Conclusions

The Chaitén samples analysed for this report are the first rhyolitic samples to be analysed by mineralogical and geochemical techniques for respiratory health hazards. Therefore, there are no existing datasets for direct comparison with these samples. However, all of the results presented are in keeping with expectations for rhyolitic eruptions given our knowledge of the health-pertinent characteristics of other magmatic compositions. These are discussed further here:

3.1 Particle size

The Chaitén samples analysed for this report are fine-grained, containing 8.7-11.9 vol. % respirable particles (< 4 µm diameter). These figures are in keeping with other silicic eruptions although the most comparable data (Table 2.3.3) is for dome-collapse eruptions such as at the Soufrière Hills volcano, Mt St Helens or Merapi. A more similar, explosive eruption style was observed at Mt Pinatubo (1991) but the data in Table 2.3.3 show that the Pinatubo ash was slightly coarser. The finest ash analysed to date is from Vesuvius (AD79) which is substantially finer than the Chaitén ash.

For the samples analysed here, there does not appear to be a correlation between grain size and distance from the volcano in the health-pertinent fractions.

When assessing the potential health hazard of the ash, as well as grain size, the duration and quantity of exposure are also vital parameters and should be taken into account in any health assessment.

3.2 Crystalline silica content

In terms of health hazard, the crystalline silica content in the samples is in keeping with the fact that, in the early stages of the eruption, there was no opportunity for large-scale cristobalite formation through vapour-phase crystallisation or devitrification within a volcanic dome/cryptodome, as has been observed at Mt St Helens, USA and the Soufrière Hills volcano, Montserrat. In this case, the presence of cristobalite may be related to crystallisation from hydrothermal fluids and incorporation of hydrothermally-altered rock, rather than primary magmatic effects. The quartz is likely to be a magmatic component.

However, lava dome growth began shortly after the initial eruption and reports indicate that dome growth continues today. We therefore recommend that crystalline silica content is re-assessed should ash be generated from a dome-collapse or explosion of dome material in the future. Crystalline silica contents from rhyolitic, as opposed to andesitic/dacitic, domes has not previously been studied.

3.3 Surface reactivity

The results of the surface reactivity and surface area experiments are in line with previously published results⁷. The data reported here suggest that the volcanic ash might represent a respiratory hazard which is not related to the crystalline silica content.

3.4 Differences among samples

All of the Chaitén samples analysed gave consistent analytical results with the exception of sample Chai_02, collected from Jacobaci. This sample had a slightly different composition to the other samples, being slightly depleted in SiO₂ and Na₂O and enriched in Fe₂O₃, MgO, CaO and SO₃. It is possible that this is as a result of minor incorporation of hydrothermally-altered minerals such as gypsum or anhydrite (CaSO₄). However, this sample also varied from the others in several significant ways: 1) the sample contained substantially elevated quantities of cristobalite and quartz; 2) it had a higher surface area than the other samples; 3) it released more iron (potentially much more Fe²⁺) than the other samples; 4) however, its surface reactivity was reduced in comparison to the other samples. We do not have any further information about the circumstances of deposition of this sample except that we assume it fell from the same eruption plume as Chai_01-06, erupted on 2 May 2008. However, the sample was collected at a much greater distance from the volcano than the other samples and it is possible that the aerodynamic properties of less-dense minerals (e.g. crystalline silica) could account for the enrichment of crystalline silica phases in this sample (as discussed by Horwell et al. 2001⁶). One might also expect to see a commensurate enrichment of fine material with distance, but this is not observed here.

3.4 Future hazard

Future eruptions from Chaitén may continue as present but may also switch to a dome-related eruption style (e.g. collapse of the lava dome or explosions which disintegrate the lava dome). In this case we strongly recommend a reassessment of the hazard, in particular the grain size and crystalline silica content of the ash.

It is also possible that Chaitén volcano might progress to a more cataclysmic rhyolitic caldera-forming eruption. This would pose a significant ashfall hazard to populations at potentially greater distances (depending on wind direction) than we have currently observed. In this case we would expect the ash to be more fine-grained due to the increased explosivity of the eruption.

We do not anticipate that surface reactivity results would alter substantially with a change in eruption style (as long as the products are rhyolitic).

3.5 Health message

The Chaitén ash is sufficiently fine to have the potential to trigger asthma attacks in susceptible people, and aggravate respiratory symptoms in people with chronic lung problems. All people should wear masks in situations where exposure to the ash is going to be high, e.g., dry, windy days and where heavy traffic or tasks such as ash removal create dust in the air.

In public health terms, the potential for the development of long-term respiratory problems depends mainly upon the amount of crystalline silica in the ash and proportion of the ash which can be easily breathed into the deep parts of the lung. Taking these results into account (see sections 2.3 and 2.5), and the experience acquired from other volcanoes over the last 25 years, the health hazard is low unless frequent eruptive activity commences which repeatedly exposes the population to high ash levels over long durations. In this case, careful monitoring of exposure and ash composition is required to make a full risk assessment.

3.6 Conclusions and suggested further work

The results of this study have found that the volcanic products from Chaitén volcano are rhyolitic, containing fine-grained, respirable particles.

The samples all contained some crystalline silica but not as much as has been observed at dome-forming volcanoes. However, the hazard from the fine-grained, crystalline silica particles must be considered with respect to the duration of exposure of populations to these particles, which may be prolonged. The samples had low surface areas and generated low quantities of hydroxyl radicals.

4. Further Information

The International Volcanic Health Hazard Network (IVHHN) is the umbrella organisation for people interested in the health effects of volcanic emissions.

Please refer to the IVHHN pamphlet on the health hazards of volcanic ash (available in Spanish) in order to learn more on the potential respiratory hazard posed by the Chaitén ash.

Please also see the IVHHN Guidelines on Recommended Dust Masks.

All information can be found and downloaded from www.ivhhn.org including a copy of this report.

5. Acknowledgments

This work was funded through a UK Natural Environment Research Council (NERC) Urgency Grant NE/G001561/1.

The authors of the report wish to thank the following contributors:

Dr Peter Baxter, Institute of Public Health, University of Cambridge, UK
for providing the health assessment and message.

Mr Chris Rolfe, Geography Department, University of Cambridge, UK
for carrying out rapid grain size analyses.

Mr Nick Marsh, Department of Geology, University of Leicester, UK
for the XRF analysis.

Prof. Bice Fubini, Dr Maura Tomatis, Dr Ivana Fenoglio and Dr Francesco Turci, Università degli Studi di Torino, Italy
for guidance and help carrying out the surface reactivity analyses.

Dr. Gordon Cressey and Dr. Hazel Hunter, Department of Mineralogy, Natural History Museum, London
for method development, support and advice during the XRD analysis.

Prof. Ken Donaldson, MRC Centre for Inflammation Research at the University of Edinburgh, for advice on particulate toxicity.

Dr Neil Cameron and PhD students for help and advice during BET analysis.

Appendix

IAS quantitative phase analysis of volcanic ash by XRD: method testing and validation

A.1 Introduction

X-ray Diffraction (XRD) is a common tool for determining and quantifying mineral assemblages in powdered samples and has been used as the method of choice for determining crystalline silica content in volcanic ash samples. Until now, however, quantitative determination of mineral phases in a heterogeneously composed dust has been problematic, particularly if the mineral assemblage is not known in advance, as matching standards are required for identification purposes.

Commonly, the Rietveld method is used for quantitative phase analysis of pure samples¹⁸ but this requires a detailed prior knowledge of the chemistry and structural form of all of the phases within the sample, therefore rendering this technique unusable for volcanic ash samples.

A major shortcoming of XRD has been the fact that plagioclase feldspar, a dominant mineral in volcanic ash assemblages, has a spectral peak which overlaps with cristobalite. To combat this, until recently, prior to XRD analysis all mineral phases except crystalline silica were removed by the Talvitie method¹⁹ which involves boiling ash in phosphoric acid to remove silicates and other minerals. However, this method is considered unreliable as the small silica crystals can undergo cation substitution (Al and Na for Si) as the other silicate minerals disintegrate within the Talvitie solution²⁰. Also the technique easily introduces error by a) boiling for too little time, thereby not dissolving all the silicates or b) boiling for too long, thereby dissolving the crystalline silica itself.

Recently, several innovations have allowed great advances in our ability to quantify minerals within heterogeneous samples. Firstly, a new style of X-ray Diffractometer is on the market which uses a curved 120° 2θ position-sensitive detector (XRD-PSD) in static geometry relative to the beam and sample. With this high-resolution instrumentation it is possible to deconvolve the main peak for cristobalite from overlapping peaks of plagioclase, thereby negating the Talvitie method.

Secondly, two new techniques for quantitative phase analysis have been pioneered by Dr Gordon Cressey at the Natural History Museum, London. The first is a whole-pattern peak-stripping method²¹. This involves matching the XRD patterns of individual phases to the multiphase sample XRD pattern. This can be done by matching previously collected XRD patterns from standards²² or utilizing digitized computational data to peak identify and quantify the phases. However, there are problems in estimating the proportion of a phase from the XRD pattern peak intensities with low resolution (old-style) XRD instruments. In addition, one still needs to know that composition of the sample in advance in order to match the major peaks with standards. This process is time consuming and is not ideal when samples of volcanic rock and/or ash need to be analyzed rapidly to determine the proportion of hazardous phases.

For this report, we have employed a new technique called the internal attenuation standard (IAS) method which has been recently developed by G. Cressey. The IAS method involves less sample preparation and processing and is, therefore, faster than the peak-stripping method or any other previously-tested quantification technique. It involves the sole quantification of the phase/phases of interest e.g. cristobalite and quartz without the need to know the mineral composition of the rest of the sample. This obviously represents a great improvement on previous methodologies and finally allows us to be able to rapidly and accurately quantify crystalline silica in volcanic ash samples.

Over recent months the IAS method has been tested and validated at the Natural History Museum, London by G. Cressey and J. Le Blond (publication in prep.). Here we summarise these results with inclusion of specific results to emphasise the validity of the technique for volcanic ash samples.

A.2 Method

The IAS method relies on the introduction of a known quantity of standard (of a compound not found in the sample) into the powder. There are a variety of materials that can be used as the internal standard in the IAS method. However, it is best to choose a compound that is likely to have a similar attenuation coefficient and peaks within the 2θ range of the sample. In these experiments ZnO was used. The IAS method involves analyzing the sample by XRD-PSD, then adding a known wt. % of the internal standard and running the mixture again on the XRD-PSD. The pure phase internal standard is also run alone (i.e. the ZnO) in addition to the standard/s for the mineral/s to be quantified e.g. cristobalite. The user then fits the ZnO to the mix + ZnO pattern, either by-eye or using a least squares fitting programme. The true value for the proportion of ZnO is known so it can be used to proportion the peak heights for the mineral/s in question. As with the peak-stripping method, all of the samples must be run for equal timescales and on the same day to avoid any change in the instrumentation conditions (i.e. flux).

Experiments were done on an Enraf-Nonius X-ray diffractometer with Inel curved position-sensitive detector (PSD). The XRD-PSD, in combination with anode blades (instead of the typical anode wire), enables rapid, high precision, high-resolution diffraction data acquisition throughout the angle ranges of 0 to $120^\circ 2\theta$. This effectively reduces the chances of phase overlap in the resulting phase XRD pattern by displaying the whole 2θ angle array.

Two experiments were devised in order to test the robustness of the IAS method:

1. Ten synthetic samples were made up from **known combinations** of four pure mineral phases chosen to represent problematic constituents of volcanic ash. Standards were gathered from the mineral collections at the Natural History Museum, London. The synthetic samples contained up to four known mineral phases (cristobalite, hematite, labradorite, obsidian) in known weight percentages. Hematite was chosen because its Fe content will cause fluorescence and raise the background level of the counts artificially. Labradorite (plagioclase feldspar) was chosen because it has 2θ values close to those of cristobalite. Obsidian, a volcanic glass, was included as the XRD pattern for amorphous materials forms a characteristic ‘hump’ in the background counts that can interfere with small intensity 2θ peaks. The synthetic mixtures of

minerals were quantified using both the whole-pattern peak-stripping method and the IAS method for comparison.

- Two samples of volcanic ash from the Soufrière Hills volcano, Montserrat were studied using the IAS method. These had been previously been quantified using the peak-stripping method by G. Cressey.

A.3 Results

Synthetic samples

Table A.3.1. gives the cristobalite quantities determined for synthetic mixtures by the IAS and peak-stripping methods. Figure A.3.1. shows the XRD spectra for one of the synthetic mixtures, for information.

Table A.3.1. Results from the quantification of cristobalite in the ten synthetic sample mixtures, by the IAS method and the peak-stripping method.

Cristobalite wt. %		
Known values (measured into the mixture)	IAS method	Peak-stripping method
0.0	0.0	0.0
5.2	5.1	6.7
10.1	10.4	9.3
10.8	13.0	12.6
11.0	9.7	10.5
16.4	15.4	18.3
19.3	20.6	19.2
25.0	22.7	25.9
33.3	32.5	35.3
39.5	40.1	39.3

Both the IAS method and the peak-stripping method gave cristobalite wt. % values within the errors expected (i.e. within 1 to 3 wt. %). This expected error takes into account any user-handling and processing errors and is based on experience. It must be remembered, however, that samples must be adequately mixed with the internal standard during the procedure and replication may be challenging due to sample inhomogeneity.

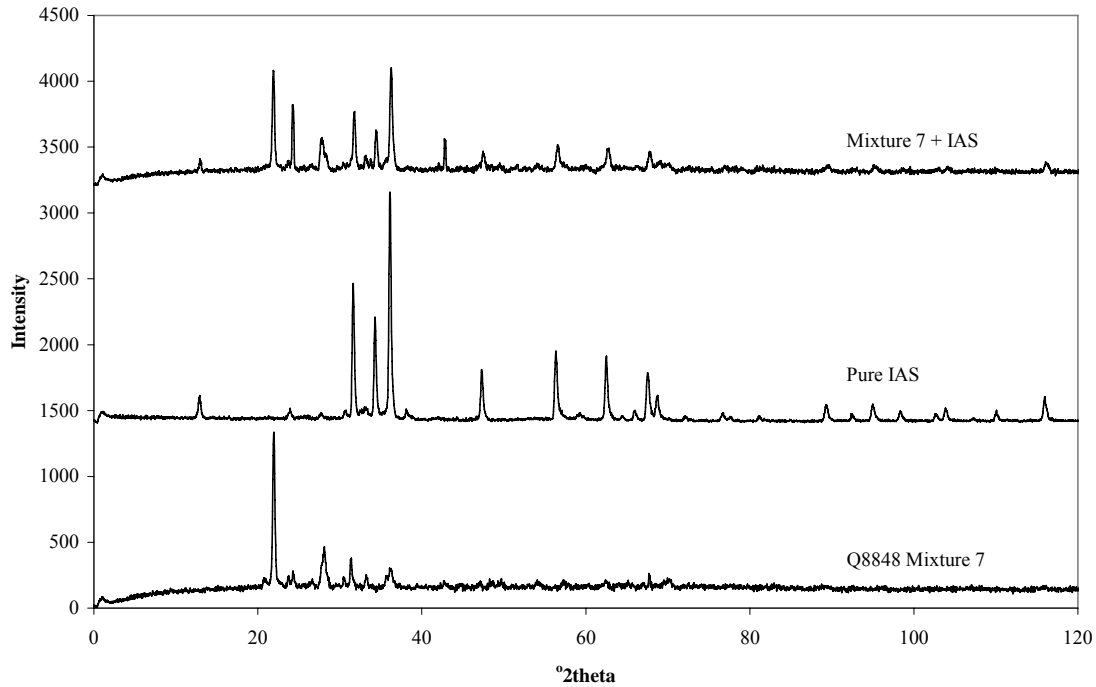


Figure A.3.1. The XRD patterns for one of the synthetic mixtures (Mix 7).

Volcanic ash samples

Table A.3.2 gives results for the Soufrière Hills volcano ash samples (labelled TWO and FOUR) analysed for cristobalite content by the IAS method here and compared with the peak-stripping data previously obtained by G. Cressey (shown in Figure A.3.2).

The IAS method gave almost identical wt. % cristobalite values to those found by the peak-stripping method some years earlier.

Table A.3.2. Cristobalite quantities for the Soufrière Hills volcanic ash samples, calculated from both the new IAS method and the whole-pattern peak-stripping method.

Sample	Cristobalite wt. %	
	IAS	Peak-stripping
TWO	17.9	18.2
FOUR	15.7	15.8

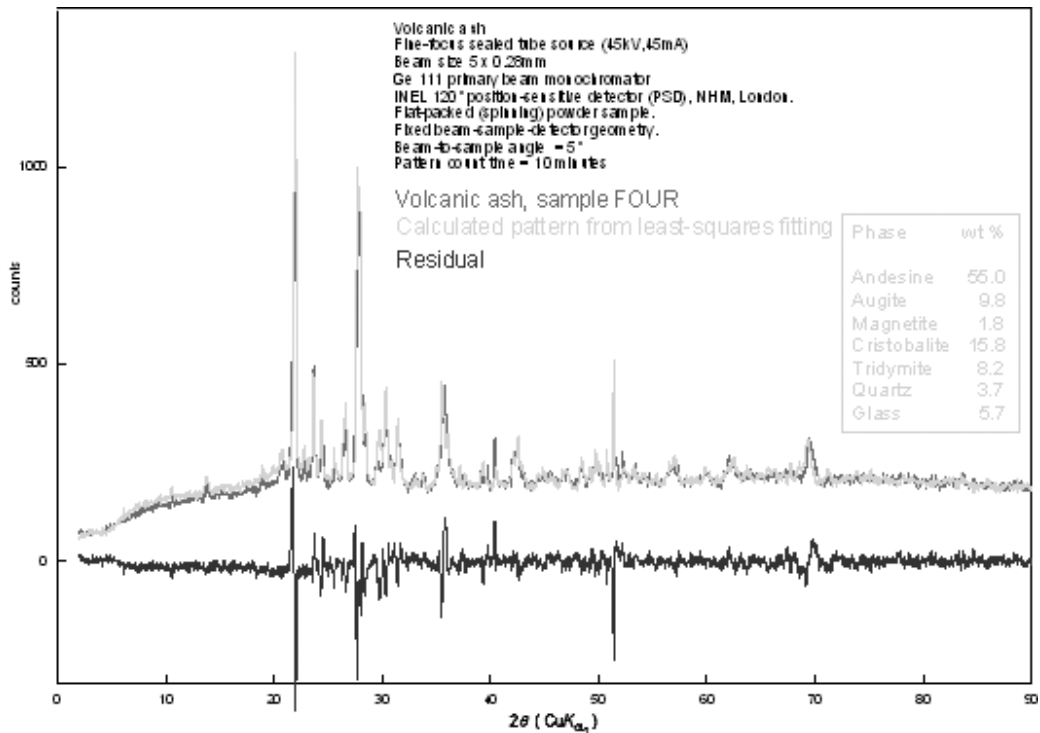


Figure A.3.2. The XRD spectra from the whole-profile peak-stripping method (by G. Cressey) of sample FOUR.

A.4. Discussion and Conclusion

The IAS method has been shown here to be robust, allowing accurate replication of results from an accepted peak-stripping method as well as from known quantities of synthetic sample. We are confident of applying the IAS method to the Chaitén samples.

References

1. Stern, C.R. Active Andean volcanism: its geologic and tectonic setting. *Revista Geológica de Chile* **31**, 161-206 (2004).
2. Le Bas, M.J. & Streckeisen, A.L. The IUGS systematics of igneous rocks. *J. Geol. Soc. Lond.* **148**, 825-833 (1991).
3. Horwell, C.J. Grain size analysis of volcanic ash for the rapid assessment of respiratory health hazard. *J. Environ. Monitor.* **9**, 1107 - 1115 (2007).
4. International Agency for Research on Cancer. *Silica, some silicates, coal dust and para-aramid fibrils* (International Agency for Research on Cancer, Lyon, 1997).
5. Horwell, C.J. & Baxter, P.J. The respiratory health hazards of volcanic ash: a review for volcanic risk mitigation. *Bulletin of Volcanology* **69**, 1-24 (2006).
6. Horwell, C.J., Braña, L.P., Sparks, R.S.J., Murphy, M.D. & Hards, V.L. A geochemical investigation of fragmentation and physical fractionation in pyroclastic flows from the Soufriere Hills volcano, Montserrat. *J Volcanol Geotherm Res* **109**, 247-262 (2001).
7. Horwell, C.J., Fenoglio, I. & Fubini, B. Iron-induced hydroxyl radical generation from basaltic volcanic ash. *Earth Plan. Sci. Lett.* **261**, 662-669 (2007).
8. Hardy, J.A. & Aust, A.E. Iron in asbestos chemistry and carcinogenicity. *Chem Rev* **95**, 97-118 (1995).
9. Kane, A.B. Mechanisms of Mineral Fibre Carcinogenesis. in *Mechanisms of Fibre Carcinogenesis* (ed. A.B. Kane, P. Boffetta, R. Saracci & J.D. Wilburn) 11-34 (International Agency for Research on Cancer, Lyon, 1996).
10. Smith, K.R. & Aust, A.E. Mobilization of iron from urban particulates leads to generation of reactive oxygen species in vitro and induction of ferritin synthesis in human lung epithelial cells. *Chem Res Toxicol* **10**, 828-834 (1997).
11. Ghio, A.J., *et al.* Role of surface complexed iron in oxidant generation and lung inflammation induced by silicates. *American Journal of Physiology* **263**, 511-517 (1992).
12. Fubini, B. & Otero Arean, C. Chemical aspects of the toxicity of inhaled mineral dusts. *Chem Soc Rev* **28**, 373-381 (1999).
13. Fubini, B. & Hubbard, A. Reactive Oxygen Species (ROS) and Reactive Nitrogen Species (RNS) generation by silica in inflammation and fibrosis. *Free Rad. Biol. Med.* **34**, 1507-1516 (2003).
14. Horwell, C.J., Fenoglio, I., Ragnarsdottir, K.V., Sparks, R.S.J. & Fubini, B. Surface reactivity of volcanic ash from the eruption of Soufrière Hills volcano, Montserrat, with implications for health hazards. *Environmental Research* **93**, 202-215 (2003).
15. Shi, X., *et al.* Generation of reactive oxygen species by quartz particles and its implication for cellular damage. *Applied Occupational and Environmental Hygiene* **10**, 1138-1144 (1995).
16. Fubini, B., Mollo, L. & Giamello, E. Free radical generation at the solid/liquid interface in iron containing minerals. *Free Rad Res* **23**, 593-614 (1995).
17. Fubini, B., Fenoglio, I., Elias, Z. & Poirot, O. Variability of biological responses to silicas: effect of origin, crystallinity, and state of surface on generation of reactive oxygen species and morphological transformation of mammalian cells. *J Environ Pathol Tox* **20**, 95-108 (2001).
18. Hill, R.J. & Howard, C.J. Quantitative phase analysis from neutron powder diffraction data using Rietveld method. *J. App. Crystal.* **20**, 467-474 (1987).

19. Talvitie, N.A. Determination of quartz in presence of silicates using phosphoric acid. *Anal. Chem.* **23**, 623-626 (1951).
20. Deer, W.A., Howie, R.A. & Zussman, J. *An introduction to the rock forming minerals* (Longman Scientific and Technical, New York, 1996).
21. Cressey, G. & Schofield, P.F. Rapid whole-pattern profile-stripping method for the quantification of multiphase samples. *Powder Diffraction* **11**, 35-39 (1996).
22. Smith, D.K., *et al.* Quantitative X-ray powder diffraction method using the full diffraction pattern. *Powder Diffraction* **2**, 73-77 (1987).